6-15-2013

Study of the thermodynamics of chromium(III) and chromium(VI) binding to iron(II/III)oxide or magnetite or ferrite and magnanese(II) iron (III) oxide or jacobsite or manganese ferrite nanoparticles

Steven Luther

Nathan Brogfeld

Jisoo Kim

Jason Parsons
The University of Texas Rio Grande Valley, jason.parsons@utrgv.edu

Recommended Citation

Luther S, Brogfeld N, Kim J, Parsons JG. Study of the thermodynamics of chromium(III) and chromium(VI) binding to iron(II/III)oxide or magnetite or ferrite and magnanese(II) iron (III) oxide or jacobsite or manganese ferrite nanoparticles. J Colloid Interface Sci. 2013;400:97-103. doi:10.1016/j.jcis.2013.02.036

Published in final edited form as:
J Colloid Interface Sci. 2013 June 15; 400: 97–103. doi:10.1016/j.jcis.2013.02.036.

Study of the Thermodynamics of Chromium(III) and Chromium(VI) Binding to Fe_3O_4 and $MnFe_2O_4$ nanoparticles

Steven Luther, **Nathan Brogfeld**, **Jisoo Kim**, and **J.G. Parsons***
The University of Texas Pan-American Department of Chemistry 1201 W University Dr. Edinburg TX 78539

Abstract

Removal of chromium(III) or (VI) from aqueous solution was achieved using Fe_3O_4, and $MnFe_2O_4$ nanomaterials. The nanomaterials were synthesized using a precipitation method and characterized using XRD. The size of the nanomaterials was determined to be 22.4 ± 0.9 nm (Fe_3O_4) and 15.5 ± 0.5 nm ($MnFe_2O_4$). The optimal binding pH for chromium(III) and chromium(VI) were pH 6 and pH 3. Isotherm studies were performed, under light and dark conditions, to determine the capacity of the nanomaterials. The capacities for the light studies with $MnFe_2O_4$ and Fe_3O_4 were determined to be 7.189 and 10.63 mg/g, respectively, for chromium(III). The capacities for the light studies with $MnFe_2O_4$ and Fe_3O_4 were 3.21 and 3.46 mg/g, respectively, for chromium(VI). Under dark reaction conditions the binding of chromium(III) to the $MnFe_2O_4$ and Fe_3O_4 nanomaterials were 5.74 and 15.9 mg/g, respectively. The binding capacity for the binding of chromium(VI) to $MnFe_2O_4$ and Fe_3O_4 under dark reaction conditions were 3.87 and 8.54 mg/g, respectively. The thermodynamics for the reactions showed negative ΔG values, and positive ΔH values. The ΔS values were positive for the binding of chromium(III) and for chromium(VI) binding under dark reaction conditions. The ΔS values for chromium(VI) binding under the light reaction conditions were determined to be negative.

Keywords

Chromium(III); Chromium(VI); binding capacity; metal oxide nanomaterials; thermodynamics

1. Introduction

The removal of chromium from drinking water is critical to global health. Chromium is not biodegradable, and accumulates in living organisms causing various diseases [1]. Water insoluble chromium(III) compounds are normally not considered a health hazard, but some studies indicate that high concentrations of chromium(III) in cells can lead to DNA damage [2]. The toxicity and carcinogenic properties of chromium(VI) have been well documented [3]. The acute toxicity of chromium(VI) is due to its oxidative properties. After chromium(VI) reaches the blood stream it can potentially damage the kidneys, liver, and/or blood cells by various oxidative reactions [4]. Through chromium(VI) is toxic to most living organisms it has many industrial applications such as wood preservation, leather tanning, and metal plating.

*Corresponding Author: Phone (956)665-7462 parsonsjg@utpa.edu.

Humans are exposed to chromium through their intake of food, drinking water, and inhalation of air containing chromium with an estimated intake of 0.01–0.03 μg (0.14 μg of chromium(VI) being the toxic limit [5]). The EPA reports that 29 million pounds of chromium is released by in rainwater, and almost 100,000 pounds of chromium is released from surface water discharges per year [6]. Chromium compounds occur naturally in the environment due to the erosion of certain rocks containing chromium, and due to volcanic eruptions. Industries such as electroplating, leather tanning, metal finishing, and chromate preparation contribute to pollution of our waterways [7, 8]. In addition, chromium occurs as a pollutant in the effluent water of coal fired electric plants as well as in the production of corrosion resistant materials [9].

A significant amount of research has been done in the effort of removing chromium from aqueous solutions, with drawbacks ranging from the subjective methods used in the environmental disposal of chemical compounds following removal of the chromium as well as the overall cost of the removal method. Methods such as membrane separation, chemical precipitation, electro-deposition, and adsorption have been utilized in the effort of removing chromium from aqueous solutions [9]. In addition, reverse osmosis and ion exchange have been somewhat successful methods, but high maintenance and operation costs are drawbacks in these methods.

Adsorption is low cost alternative as it is simplistic, many different materials have been investigated such as agricultural material such as rice straw, wool, coconut husks, peat mosses, and industrial waste rubber tires, have been tested in the adsorption of chromium [10]. These absorbents have not been able to meet discharge standards alone and generate large amounts of secondary waste. How to separate the adsorbents from the solution in a reasonable amount of time is another significant challenge to overcome in the adsorption process [7]. Activated carbon is also a well known and efficient adsorbent, but its high cost and difficulty of manufacturing restricts its use in most environments. Much research into various adsorbents such as clay minerals, metal oxides, and organic polymers has been performed with limited success in removal of chromium from our waterways, but continued efforts are being exerted [11]. Magnetic adsorbents offer a promising solution to the challenge of separating the adsorbents from solution, as the separation can be performed quite effectively by the application of a magnetic field [7]. Utilizing this method could reduce the problem of excess environmental waste in the cleanup of our waterways [7].

Interest has grown, and research time has been extended in the study of nano-sized materials to remove chromium from aqueous solutions because of the material’s unique physical and chemical properties, and the research is indicating promising results. These nanomaterials, with high aspect ratios, have been exploited in numerous unique applications especially in relation to the removal of heavy metals [12]. The surface atoms of a nanoparticle are unsaturated, and thus they can bind other atoms that possess a high chemical affinity (12). Chromium binding is a significantly surface area dependent process, and thus the increased surface area relative to the mass of an element such as iron aids in accelerating the reduction rate. There is substantiated evidence that nano-sized metal particles are more reactive than commercial powders likely because of increased surface area and accelerated surface reactivity [13]. The sorption of toxic elements to different nanomaterials has been studied in the literature and has shown much promise as an emerging technology for water cleaning (14–44). In addition, thermodynamic studies have been performed to help elucidate the binding mechanism for chromium binding to different nanomaterials (28–38). In general the mechanism for metal binding to nanomaterials is through one of three different types 1.) dissolution and coprecipitation; 2.) ion exchange mechanism; and 3.) physisorption. (28–38)

In this study, nanoadsorbents Fe_3O_4 and $MnFe_2O_4$ were synthesized and evaluated for their ability to remove chromium from aqueous solutions. The $MnFe_2O_4$ nanomaterial were synthesized by mixing iron (II) chloride and manganese(II) sulfate in water, then using a precipitation method consisting of a slow titration with sodium hydroxide. The Fe_3O_4 nanomaterial was also synthesized using a precipitation method, that consisted of a slow titration with sodium hydroxide into a solution of iron(II). The synthesized iron oxide nanomaterials were tested for the removal of chromium(III) and (VI) from aqueous solution. The iron oxide nanoparticles were characterized using X-ray diffraction, which showed the Fe_3O_4 and $MnFe_2O_4$ nanoparticles had crystal structures of magnetite and jacobsite, respectively. Batch studies were performed to determine the optimum pH for binding using 300 ppb of either chromium(III) or (VI), from pH 2 to pH 10. Isotherm studies were performed to determine the capacities of the iron oxide nanomaterials for chromium(III) and (VI). In addition, thermodynamic studies were performed to evaluate the binding capability at various temperatures as well as the sensitivity to light of the binding.

2. Methodology

2.1 Synthesis of nanoadsorbents

1.0 L solutions of both 30 mM Fe(II) (from $FeCl_2$) and 30 mM Fe(III) (from $FeCl_3$) were prepared, then each slowly titrated with 90 mL of 1.0M NaOH for approximately 4 hours ultimately obtaining a 1:3 ratio of M^{n+}:OH^-. A solution of of 20 mM Fe(II) (from $FeCl_2$) and 10 mM Mn(II) (from $MnCl_2$) was also prepared and titrated in the same fashion. The long titration time was utilized to inhibit the formation of large particles in the solution. Each solution was then heated to 100° C for 1 hour, the subsequently cooled to room temperature. Once cool, the solutions were then centrifuged at 3,000 RPM, and rinsed three times with ultra-pure water (18 MΩ) in order to remove any excess reagents or byproducts that may have formed.

2.2 XRD characterization

Rigaku Miniflex II system with a scintillation detector was used to acquire X-ray powder diffraction patterns using the Cu K_α The scans were acquired from 20 to 60 in 2θ with a counting rate of 2 seconds and a step of 0.02° in 2θ. The phase of the Fe_3O_4, Fe_2O_3 and $MnFe_2O_4$ nanomaterials that were synthesized was determined from the acquired XRD patterns after they were fitted and background corrected using the Le Bail fitting protocol. The average grain size of each of the nanomaterials was then determined using Scherrer's equation. The size analysis was performed using the full width half maximum (FWHM) of at least three independent diffraction peaks for the Fe_3O_4 and $MnFe_2O_4$ nanomaterials.

2.3 pH profile

Chromium(III) and chromium(VI) binding was tested at pH 2–10 to the nanoadsorbents. 300 ppb solutions of each chromium(III) and chromium(VI) were prepared and pH adjusted using dilute sodium hydroxide and/or dilute nitric acid. 4.0 mL of the pH adjusted solutions was added to 5.0 mL test tubes which contained 10 mg of dry nanomaterial. The test tubes were then capped, and equilibrated on a rocker for one hour. Control test tubes containing 4 mL of each pH adjusted chromium(III) and chromium(VI) were ran with each equilibration scenario. Test tubes were tested in triplicate for statistical analysis. Following equilibration, each set of test tubes was centrifuged at 3000 RPM for five minutes, and the supernatant from each tube was collected for analysis. The supernatants were then analyzed with a Perkin Elmer AAnalyst 800 using Furnace Atomic Absorption Spectroscopy (FAAS) in order to determine the amount of either chromium(III) or chromium(VI) remaining following binding to the nanomaterials. Calibration curves with correlation coefficients (R^2) of 0.99 or better were used in the analysis.

2.4 Capacity studies

A pH of 6 was determined to be the optimum binding pH for chromium(VI), and a pH of 3 was determined to be the optimum binding pH for chromium(III). After establishing these optimum binding pH levels, capacities of the nanomaterials were evaluated using concentrated solutions of 0.3, 1, 5, 10, 25, 50, and 100 ppm of either chromium (III) or chromium (VI). These solutions were then added to test tubes containing 10 mg of dry nanomaterial. Subsequently, the test tubes were capped and placed on a rocker to equilibrate for one hour. Following the equilibration, the test tubes were then centrifuged at 3000 RPM for five minutes. The supernatants were then collected and analyzed using inductively coupled plasma-optical emission spectroscopy (ICP-OES) in order to detect the level of chromium remaining in solution after binding. The 50 and 100 ppm chromium solutions were diluted to 20 ppm prior to analysis. Each set was ran with control samples that were prepared in the same manner as the samples. Each sample was ran in triplicate for statistical purposes. Calibration curves with correlation coefficients (R^2) of 0.99 or better were obtained for the analysis.

2.5 Thermodynamic studies

Thermodynamic studies were conducted at the optimum binding pH of 6 for chromium(III) and pH 3 for chromium(VI). Solutions containing 20ppm of either chromium(III) or Chromium(VI) were pH adjusted accordingly, added to test tubes (which contained 10 mg of nanomaterial), and capped. Once in test tubes, the sets of each nanoadsorbent were then equilibrated on rockers at various temperatures: 323 K, 293 K, and 277 K. The procedure was performed under both light and dark reaction conditions for one hour. Following equilibration, the test tubes were centrifuged at 3,000 RPM for five minutes, and the supernatants were then collected and analyzed using inductively coupled plasma-optical emission spectroscopy (ICP-OES) in order to determine the concentration of chromium still present in solution after binding. Each sample was ran in triplicate for statistical purposes and verified against controls. Calibration curves with correlation coefficients (R^2) of 0.99 or better were utilized in the evaluation.

2.6 Chromium Analysis

2.6.1 ICP-OES Analysis—ICP-OES analysis was performed using a Perkin Elmer Optima 8300 DV ICP-OES. The operation parameters are shown in Table 1. The calibrations were performed from 0.01 ppm to 20 ppm using a minimum of 4 standards plus a blank solution. In addition, any samples over the calibration range were diluted to work within the defined calibration range. All calibration curves obtained had correlation coefficients of 0.99 or better.

2.6.2 FAAS Analysis—Chromium analysis was performed using a Perkin Elmer AAnalyst 800 in Flame mode. The instrument was used under the following conditions: wavelength for analysis of 357.9 nm, a fuel mixture of 17.0: 2.5 (air: acetylene), a read time of 3 seconds, and a high efficiency nebulizer was utilized for the chromium analysis. Furthermore, all standards, controls, and reaction samples were read in triplicate for statistical purposes.

3. Results and Discussion

3.1 XRD

Figure 1A and B show the diffraction patterns of the synthesized Fe_3O_4 and $MnFe_2O_4$, nanomaterials, respectively. From the Lebail Fitting of the diffraction patterns which showed the 220, 311, 222, 400, 422, 333 and 511 diffraction peaks, which indicating that the

materials are Fe_3O_4 and $MnFe_2O_4$ (14). Additionally, using the Scherr's analysis of three independent diffraction peaks it was determined that the average gain size of the nanomaterials was 22.4 ± 0.9 and 15.5 ± 0.5 nm for the Fe_3O_4 and $MnFe_2O_4$ nanomaterials, respectively. Furthermore, the synthesis technique also shows small particle size distribution as is indicated by the small errors on the size. This is in good agreement with diffraction data obtained by Parsons *et al* using a similar synthesis technique (14). In addition, the similarity of the grain sizes between the two materials (within 5 nm) should minimize nanoparticle size effects in the data. The small change in particle size between the two nanomaterials should only show differences in material behavior for the sorption studies.

3.2 pH Studies

Figure 2 A and B show the pH binding profile for chromium(VI) and chromium(III) binding to the Fe_3O_4 and $MnFe_2O_4$ nanomaterials from pH 2 through pH 10. As can be observed in Figure 2 A, the chromium(VI) binding decreases with increasing pH from 80–90% binding at pH 2 to approximately 0 at pH 7 and above. However, the binding of chromium(III) to the metal oxide nanomaterials is low a pH 2 and increase sharply between pH 3 and 4, and then remains relatively constant ranging from 80–90% for the Fe_3O_4 up to pH 10. Whereas, the binding of the chromium(III) to the $MnFe_2O_4$ maximizes at approximately pH 6, with 80% binding, and then decreases slowly to approximately 60% binding at pH 10. Similar binding has been observed for chromium(III) and chromium(VI) binding to other metal oxide nanomaterials (16–40). Iron oxide coated sand showed a similar binding trend higher adsorption at low pH and a reduced binding as pH was increased (16) Another study showed similar pH dependency of chromium(VI) binding to a low cost dolomite adsorbent with very high binding at low pH and decreasing binding at higher pH (17). Studies with activated carbon show the binding of chromium (VI) from solution high at pH 2 reaching approximately 90% and the binding decreased with increasing pH (18). Similarly, in the sorption of chromium(VI) on to polyacrylamide grafted sawdust a higher binding of chromium(VI) was observed at low pH and the binding was found to decrease with increasing pH (19). High binding of chromium(VI) at low pH has also been noted for the binding of chromium(VI) to both akaganeite and synthetic hematite and decreased with increasing pH (20,). The opposite trend has been observed when chromium(VI) binds to clay materials (21). However, a recent study by Lv *et al* showed that at pH 8 the sorption of chromium(VI) effective binds to zerovalent iron-Fe_3O_4 nanomaterials (22). The observed binding was approximately 96% of a 20 ppm solution. In this study it was also shown that 2hrs of contact time was necessary for binding (22).

3.3 Capacity Studies

The capacity studies for the binding of both chromium(III) and chromium(VI) are shown in Tables 2 and 3, for light and dark conditions respectively. The binding capacities of the two nanomaterials for chromium ions were determined using isotherm studies at 23°C. Additionally, the binding was found to follow the Langmuir isotherm model. It can be seen in Table 3 (the data obtained from the experiment under conditions of light) that chromium(III) had much higher observed binding capacities to both the Fe_3O_4 and $MnFe_2O_4$ nanomaterials than chromium(VI). The observed binding capacity of the chromium(III) was more than twice the observed capacity of chromium(VI) to the same nanomaterial. The Fe_3O_4 showed higher binding of both chromium(VI) and chromium(III) than the $MnFe_2O_4$ nanomaterial under both the light and dark conditions. In addition, the binding capacities of the Fe_3O_4 nanomaterials are higher than the $MnFe_2O_4$ nanomaterial under the dark conditions, as can be seen in Table 3. The $MnFe_2O_4$ binding capacity for chromium(III) was only found to be lower by approximately 1.5 mg/g under dark conditions compared to light conditions. This difference in the binding under light and dark conditions may be related to the surface chemistry and the interaction of light with the surface of the

material and the chromium ions. The binding of metal ions to nanomaterials is affected by the surface charge of the nanomaterial, which could be affected by the presence or absence of light. The noted increas in capacity under the dark reaction condition may be a synergistic effect of surface charge and the absence of light.

It has been shown in the literature that Fe_2O_3 has a higher binding capacity than Fe_3O_4 materials, as does FeOOH, another iron(III) compound that has been used for chromium(VI) binding. The preparation of nanomaterial controls their reactivity and the functionality (23). In the current study, slightly lower capacities were observed compared to the literature for similar materials. However, there are many different parameters that must be taken into consideration when comparing different capacity studies. Firstly, the reaction conditions may vary dramatically between different studies. Secondly, the size of the sorbents must be taken into consideration which relates to the total surface area of the nanomaterial. Finally, thirdly other factors that contribute to varying capacities are the porosity of the material, stability of the material, and the possible effects of surfactants used in the preparation of the nanomaterial. Furthermore, the presence of a supporting material will change the binding capacity of a material. The method of preparation of the materials plays an important role in the capacity of a nanomaterial for the binding of metal ions from solution (22–26). It has been suggested in the literature that the release of high amounts of iron or manganese from these types of nanomaterials can cause increased removal efficiency for arsenic (14, 15, 41). The potential release of ions from the different sorbents may cause co-precipitation of the ions of interest, as has been mentioned by Smith and Ghiassi (45). Equilibration time also plays an important role in binding capacity, higher capacities are generally observed with longer equilibration times.

Chromium(III) is relatively non-toxic to living organisms and is in fact a micronutrient (42). Due to its low toxicity the capacities of chromium(III) are not commonly presented in the literature. The capacities for the sorption of chromium(III) to different inorganic materials ranges dramatically from 26 mg/g for zeolites to 2.3 mg/g for fly ash (27). The two nanomaterials investigated in the current study have capacities within the range of most materials currently reported.

3.4 Thermodynamic Studies

The data from the thermodynamic studies are present in Tables 4–7 for the light and dark condition reactions. The spontaneity of each reaction (Gibbs free energy change, ΔG) for the reaction was determined using the following relationship between ΔG and the distribution factor for each chromium species:

$$\Delta G = -RT\ln(K_d)$$

where R is the gas constant (8.314 $Jmol^{-1}\ K^{-1}$), K_d is the partition coefficient and T is absolute temperature (K). The thermodynamics for the sorption of chromium(III) and chromium(VI) to various materials has been shown in the literature (28). For the adsorption of chromium(III) and chromium(VI) to bentonite, the calculated ΔG at 303 K was determined to be −3.91 and −0.441 kJ/mol, respectively (28). The bentonite values were much smaller in magnitude than the values obtained in the current study. The negative ΔG values obtained in the current study indicate that the sorption of both the chromium(III) and chromium(VI) are spontaneous under both the light and dark conditions. The sorption of chromium(VI) by calcinated Mg-Al-CO_3 showed an activation energy of 40 kJ/mol (29) Whereas, the binding of chromium(VI) to ester- and alkylmodified silica surfaces resulted in Free energy of adsorption values of 37.4 ± 0.5 and 37.1 kJ/mol for alkyl- and ester-modified surfaces, respectively (30). Using α-aluminum oxide it has been determined that the ΔG

ranged from −34 to −40 kJ/mol for chromium(VI) (31). The reaction of chromium(VI) with Al_2O_3 has also showed ΔG values in approximately the same range observed in the current study from −3.72. to −4.81 (32–33). The reaction conditions were not noted whether the reactions were performed in the dark or light. Further studies on similar materials (metal oxide/ oxyhydroxide nanomaterials) showed ΔG values along the same magnitude around from −3.0 to −4.0. However, the binding of chromium(VI) to synthetic hematite showed a positive ΔG of 1.6kJ/mol at 300 K (34). The binding of chromium with Al-Mg mixed metal hydroxides have shown ΔG values of −6.26, −8.21 and −8.96 kJ/mol at 20, 30 and 40°C, respectively (8). In changing the sorbent material to a modified clay it has been shown that the ΔG value changes dramatically to approximately −40 kJ/mol (43). The higherΔG values observed with modified clay materials may be indicating that the reaction is partially through ion exchange with these types of materials. These large values for the ΔG of sorption are not observed in the current study, which indicates that a different mechanism for the binding of chromium(VI) to Fe_3O_4 and $MnFe_2O_4$ nanomaterials may be involved. It has also been suggested in the literature that ΔG_{ads} values in the ranges of −34 to −40 indicate that hydrogen bonding controls the binding of chromium(VI) to nanomaterials (31). However, when ΔG values are 18 or below the sorption is through physisorption on to the material is suggested (31). In the present study, the ΔG for chromium(VI) binding to the metal oxide nanomaterials was found to range from −6.3 kJ/mol to −11.25 kJ/mol as presented in Table 4. This range of ΔG values indicates that chromium(VI) may be through physisorption of the chromium to the metal oxide nanomaterials. The increase in the magnitude of the ΔG value with increased temperature for reaction with both the Fe_3O_4 and $MnFe_2O_4$ nanomaterials indicates that the sorption process becomes more favorable at higher temperatures and is an endothermic reaction. There was no large difference in the ΔG values between the light and dark reactions with the Fe_3O_4 nanomaterial, which indicates there is no preference in reaction under light or dark conditions. However, the $MnFe_2O_4$ nanomaterial reaction showed to be slightly more favorable under dark conditions at all temperatures than the reaction performed under light conditions.

The range of the ΔG values for the binding of chromium(III) to the metal oxide nanomaterials was much higher in magnitude from, −86 to −171 kj/mol as presented in 5. The large negative ΔG values for the binding of the chromium(III) to the metal oxide nanomaterials may be indicating that the binding is through an ion or molecular exchange mechanism, which might occur through the exchange of water molecules and protons on the surface of the nanomaterial. The reactions were performed at a pH of 4 thus the surface of the material may have had protons bound to the surface.

The enthalpy (ΔH) and entropy (ΔS) change for the reaction was evaluated utilizing the relationship between ΔG, ΔH, and ΔS:

$$\Delta G^{\circ} = \Delta H^{\circ} - T\Delta S^{\circ}$$

The above equation can be rewritten using the Ln K_d as a substitution for the ΔG of the reaction as follows:

$$\mathrm{Ln}k_d = \frac{\Delta S}{R} - \frac{\Delta H}{RT}$$

Therefore by plotting Ln K_d against 1/T (K) the slope of the line gives the ΔH of the reaction and the intercept of the plot gives the ΔS of the equation. The Thermodynamic plots of the data for both the chromium(III) and chromium(VI) binding to the nanomaterials are shown in Figure 3.

The ΔH values for the binding of chromium(VI) and chromium(III) to the Fe_3O_4 and $MnFe_2O_4$ nanomaterials are shown in Table 5. The binding of both chromium ions to the Fe_3O_4 nanomaterial showed higher enthalpies of binding under light conditions when compared to the dark conditions. The higher enthalpies of binding under light conditions indicate a slightly more endothermic reaction than under dark conditions. However, the binding of chromium(III) ions to the Fe_3O_4 nanomaterial showed to be a more endothermic reaction than the binding of chromium(VI) ions, as indicated by the higher ΔH values for the binding of chromium(III) (refer to Table 5), which has also been observed in the binding of chromium(III) and chromium(VI) binding to hydrous titanium dioxide (21). Similarly, the binding of Co(II) ions to sepiolite showed higher ΔH values for the binding of chromium(III) over chromium(VI) (21) In the current study the binding of both the chromium(III) and chromium(VI) ions to the $MnFe_2O_4$ nanomaterials showed different results when compared to the Fe_3O_4 nanomaterial. The binding of the chromium(VI) to the $MnFe_2O_4$ nanomaterial showed a higher ΔH value under dark conditions as compared to the same reaction under light conditions. The higher ΔH value, more than twice the value determined for the reaction under light conditions, indicates that the reaction is much more endothermic under dark conditions than light conditions. Similarly, the ΔH values determined for the chromium(III) binding to the $MnFe_2O_4$ also showed a ΔH value for the dark reaction conditions at least twice a large as the reaction performed in the light conditions which indicates that the reaction with chromium(III) ions is more endothermic in the dark compared to the reaction in the light with $MnFe_2O_4$. Whereas, the opposite trend is observed in enthalpy change in the binding of both the chromium(III) and chromium(VI) ions to the Fe_3O_4 nanomaterial. Furthermore, the ΔH value of the binding was below 40 kJ/mol which indicates that the binding is through physisorption as has been suggested for the binding of Chromium(VI) to zirconium oxide (35). The relatively high ΔH value for the chromium(III) binding may be indicating that the binding occurs through an exchange mechanism between the nanomaterials studied and the chromium(III) ions.

The calculated ΔS for the reaction between the chromium(VI) and the nanomaterials showed a positive value for the dark reaction conditions, refer to Table 6. Under dark conditions the reaction would indicate something is being released into solution to increase the disorder which could be a reductive dissolution of the material at the surface. Donation of electrons from the nanomaterial surface would facilitate the binding of the chromium, and reduction of the chromium(VI) to chromium (III). Reductive dissolution has been noted in the literature for the binding of higher oxidation state elements to various nanomaterials, including $MnFe_2O_4$, and Fe_3O_4 (14,36–38). Parsons, et al. have shown dissolution of $MnFe_2O_4$ and Fe_3O_4 when reacted with arsenic(III) and arsenic(V) (14). A reduction of the chromium and release of manganese into solution may explain why the dark reactions are increasing the amount of entropy in the system. However, the opposite is observed for ΔS under the light reaction conditions for both the Fe_3O_4 and $MnFe_2O_4$, a decrease in the entropy of the system was observed. A reduction in the ΔS would promote the suggestion of a physisorption type of reaction where the total number of molecules in solution is reduced after reaction. In addition, the presence of light may stabilize the manganese from oxidizing and dissolving in the presence of the chromium(VI). A reduction in the total number of molecules in solution would decrease the disorder of the solution. The ΔS for the chromium(III) binding to the Fe_3O_4 and $MnFe_2O_4$ nanomaterials all showed positive values. The positive change in entropy supports the hypothesized ion exchange mechanism for the binding of chromium(III) to the respective nanomaterials.

4. Conclusions

The binding of chromium(III) and chromium(VI) to the Fe_3O_4 and $MnFe_2O_4$ nanomaterials show opposite behavior. The chromium(VI) was found to bind to both nanomaterials higher

at low pH and decrease to no binding above pH 6.0. The chromium(III) bound very low at pH 2 and increased to a maximum around pH 6 for both nanomaterials. The isotherm studies showed the binding of both chromium(VI) and chromium(III) followed the Langmuir isotherm. In addition, the binding of both chromium species occurred at high levels making the material a viable option for the cleaning/remediation of water. The thermodynamic studies for chromium(VI) and chromium(III) showed that the reaction is spontaneous in the temperature range tested, as was indicated by the negative ΔG values obtained for all reactions. The chromium(VI) reactions under dark conditions with the $MnFe_2O_4$ showed a more negative ΔG value than the similar reaction conducted under light conditions. The Fe_3O_4 showed no preference in terms of the ΔG values under light or dark conditions. However, the chromium(III) binding to both nanomaterials showed much more negative ΔG values under the light conditions compared to the dark condition reactions. The ΔH studies indicate an endothermic reaction occurs during the binding process. ΔS was found to decrease during the binding of chromium(VI) to the nanomaterials under the light conditions and the opposite was true under the dark condition reactions. Entropy was found to increase for the reaction of chromium(III) with both nanomaterials under all reaction conditions. The thermodynamics indicate that the reaction has two different mechanisms for the binding of chromium(VI) possibly through physisortpion and through some type of exchange mechanism. However, chromium(III) more than likely binds to the nanomaterials through an exchange mechanism as the entropy was found to increase under all reaction conditions.

Acknowledgments

Authors would like to thank the NIH UTPA RISE program (Grant Number 1R25GM100866-01), NSF, URM program (grant number DBI 9034013), HHMI (grant 52007568). The Authors acknowledge financial support from the Welch Foundation for supporting the Department of Chemistry (Grant number GB-0017), and UTPA for sponsoring this research project.

References

1. Barceloux DG, Barceloux D. Chromium. Clinical Toxicol. 1999; 37(2):173–194.
2. Dayan AD, Paine AJ. Mechanisms of chromium toxicity, carcinogenicity, allergenicity: Review of the literature from 1985 to 2000. Hum. Exp. Toxicol. 2001; 2(9):439–451. [PubMed: 11776406]
3. Astmond DA, MacGregor JT, Slesinski RS. Trivalent Chromium: Assessing the Genotoxic Risk of an Essential Trace Element and Widely Used Human and Animal Nutritional Supplement. Crit. Rev. Toxicol. 2008; 38(3):173–190. [PubMed: 18324515]
4. Ghorbel-Abid I, Jradb A, Nahdia K, Trabelsi-Ayadia M. Sorption of chromium (III) from aqueous solution using bentonitic clay. Desalin. 2008; 246:595–604.
5. Lee S-M, Kim W-G, Laldawngliana C, Tiwari D. Removal Behavior of Surface Modified Sand for Cd(II), Cr(VI) from Aqueous Solutions. J. Chem. Eng. Data. 2010; 55:3089–3094.
6. Zhao Y-G, Shen H-Y, Pan S-D, Hu M-Q, Xia Q-H. Preparation characterization of amino-functionalized nano-Fe3O4 magnetic polymer adsorbents for removal of chromium(VI) ions. J. Mater. Sci. 2010; 45:5291–5301.
7. Kotas J, Stasicka Z. Chromium occurrence in the environment methods of its speciation. Environ. Pollut. 2000; 107:263–283. [PubMed: 15092973]
8. Li E, Zeng X, Fan Y. Removal of chromium ion (III) from aqueous solution by manganese oxide and microemulsion modified diatomite, Science Direct. Desalin. 2007; 238:158–165.
9. Bhutani MM, Mitra AK, Kumari R. Adsorption of Cr(VI) on Manganese Dioxide from Aqueous Solution, Microchim. Acta. 1992; 107:19–26.
10. Sevgi K. Adsorption of Cd(II), Cr(III) and Mn(II) on natural sepiolite. Desalin. 2008; 244:24–30.
11. Li Y, Gao B, Wu T, Sun D, Li X, Wang B, Lu F. Hexavalent chromium removal from aqueous solution by adsorption on aluminum magnesium mixed hydroxide. Water Res. 2009; 42(12):3067–3075. [PubMed: 19439337]

12. Xiaojun Z, Cui Y, Zhu X, Hu Z, Chang X. Preparation of morin modified nanometer SiO2 as a sorbent for solid-phase extraction of trace heavy metals from biological natural water samples. J. Mater. Sci. 2010; 45:5291–5301.
13. Rivero-Huguet M, Marshall WD. Reduction of hexavalent chromium mediated by micro- and nano-sized mixed metallic particles. J. Hazard. Mater. 2009; 169(1–3):1081–1087. [PubMed: 19446392]
14. Parsons JG, Lopez ML, Peralta-Videa JR, Gardea-Torresdey JL. Determination of arsenic(III) and arsenic(V) binding to microwave assisted hydrothermal synthetically prepared Fe_3O_4, Mn_3O_4, and $MnFe_2O_4$ nanoadsorbents. Microchem. J. 2009; 91:100–106.
15. Luther S, Borgfeld N, Kim J, Parsons JG. Removal of arsenic from aqueous solution: A study of the effects of pH and interfering ions using iron oxide nanomaterials. Microchem. J. 2012; 101:30–36.
16. Khaodhiar S, Azizian MF, Osathaphan K, Nelson PO. Copper, Chromium, and Arsenic Adsorption And Equilibrium Modeling in an Iron-Oxide-Coated Sand, Background Electrolyte System. Water, Air, and Soil pollution. 2000; 119(1–4):105–120.
17. Albadarina AB, Mangwandia C, Al-Muhtasebb AH, Walkera GM, Allena SJ, Ahmada MNM. Kinetic and thermodynamics of chromium ions adsorption onto low-cost dolomite adsorbent. Chem. Eng. J. 2012; 179:193–202.
18. Wu Y, Ma X, Feng M, Liu M. Behavior of chromium and arsenic on activated carbon. J. Hazard. Mater. 2008; 159:380–384. [PubMed: 18378074]
19. Raji C, Anirudhan TS. Batch Chromium(VI) Removal by Polyachromiumylamidegrafted Sawdust Kinetics and Thermodynamics. Water Res. 1998; 32(12):3772–3780.
20. Lazaridis NK, Bakoyannakis DN, Deliyanni EA. Chromium(VI) sorptive removal from aqueous solutions by nanocrystalline akaganeite Chemosphere. 2005; 58:65–73.
21. Kara M, Yuzer H, Sabah E, Celik MS. Adsorption of cobalt from aqueous solutions onto sepiolite. Water Res. 2003; 37:224–232. [PubMed: 12465804]
22. Lv X, Xu J, Jiang G, Tang J, Xu X. Highly active nanoscale zero-valent iron (nZVI)–Fe_3O_4 nanocomposites for the removal of chromium(VI) from aqueous solutions. J. Colloid Interface Sci. 2012; 369:460–469. [PubMed: 22177747]
23. Tel H, Alta s Y, Taner MS. Adsorption characteristics and separation of Cr(III) and Cr(VI) on hydrous titanium(IV) oxide. J. Hazard. Mater. B. 2004; 112:225–231.
24. Goswamee RL, Sengupta P, Bhattacharyya KG, Dutta DK. Adsorption of Cr(VI) in layered double hydroxides. Appl. Clay Sci. 1998; 13:21–34.
25. Mor S, Ravindra K, Bishnoi NR. Adsorption of chromium from aqueous solution by activated alumina and activated charcoal. Bioresour. Technol. 2007; 98:954–957. [PubMed: 16725320]
26. Weng C-H, Sharma YC, Chu S-H. Adsorption of Cr(VI) from aqueous solutions by spent activated clay. J. Hazard. Mater. 2008; 155:65–75. [PubMed: 18162297]
27. Bailey SE, Olin TJ, Bricka RM, Adrian DD. A Review of Potentially Low-Cost Sorbents for Heavy Metals. Water Res. 1999; 33(11):2469–2479.
28. Khan, Saad Ali; Riaz-ur-Rehman; Khan, M. Ali Adsorption of chromium (III), chromium (VI) and silver (I) on bentonite. Waste Manage. 1995; 15(4):271–282.
29. Sushanta, Debnath; Uday, Chand Ghosh. Kinetics, isotherm thermodynamics for Cr(III), Cr(VI) adsorption from aqueous solutions by crystalline hydrous titanium oxide. J. Chem. Thermodyn. 2008; 40:67–77.
30. Al-Abadleh, Hind A.; Voges, Andrea B.; Bertin, Paul A.; Nguyen, SonBinh T.; Franz, M. Geiger Chromium(VI) Binding to Functionalized Silica/Water Interfaces Studied by Nonlinear Optical Spectroscopy. J. Am. Chem. Soc. 2004; 126:11126–11127. [PubMed: 15355074]
31. Musorrafiti MJ, Konek CT, Hayes PL, Geiger FM. Interaction of Chromium(VI) with the α-Aluminum Oxide-Water Interface. J. Phys. Chem. C. 2008; 112:2032–2039.
32. A Lvarez-Ayuso E, Garcia-Sanchez A, Querol X. Adsorption of Cr(VI) from synthetic solutions and electroplating wastewaters on amorphous aluminium oxide. J. Hazard. Mater. 2007; 142:191–198. [PubMed: 16978771]

33. Sharma YC, Srivastava V, Mukherjee AK. Synthesis and Application of Nano-Al_2O_3 Powder for the Reclamation of Hexavalent Chromium from Aqueous Solutions. J. Chem. Eng. Data. 2010; 55:2390–2398.
34. Adegoke HI, Adekola FA. Equilibrium sorption of hexavalent chromium from aqueous solution using synthetic hematite. Colloid J. 2012; 74(4):420–426.
35. Alvares Rodrigues L, Maschio LJ, Evangelista da Silva R, Caetano Pinto da Silva ML. Adsorption of Cr(VI) from aqueous solution by hydrous zirconium oxide. J. Hazard. Mater. 2010; 173:630–636. [PubMed: 19748728]
36. Chiu VQ, Hering JG. Arsenic adsorption and oxidation at manganite surfaces. 1. Method for simultaneous determination of adsorbed and dissolved arsenic species. Environ. Sci. Technol. 2000; 34:2029–2034.
37. Nesbitt HW, Canning GW, Bancroft GM. XPS study of reductive dissolution of 7Å-birnessite by H_3AsO3, with constraints on reaction mechanism. Geochim. Cosmochim. Acta. 1998; 62(12): 2097–2110.
38. Banerjee D, Nesbit HW. Oxidation of aqueous Cr(III) at birnessite surfaces: constraints on reaction mechanism Geochim. Cosmochim. Acta. 1999; 63(11/12):1671–1687.
39. Zhao Y-G, Shen H-Y, Pan S-D, Hu M-Q, Xia Q-H. Preparation and characterization of amino-functionalized nano-Fe3O4 magnetic polymer adsorbents for removal of chromium(VI) ions. J. Mater. Sci. 2010; 45:5291–5301.
40. Kousalya GN, Rajiv Gandhi Muniyappan, Meenakshi S. Preparation of Modified Chitin for the Removal of Chromium(VI). Biorem. J. 2010; 14(4):208–218.
41. Ajouyeda O, Hurel C, Ammari M, Allal LB, Marmier N. Sorption of Cr(VI) onto natural iron and aluminum (oxy)hydroxides: Effects of pH, ionic strength and initial concentration. J. Hazard. Mater. 2009; 174(1–3):616–622. [PubMed: 19818554]
42. Yuan P, Fan M, Yang D, He H, Liu D, Yuan A, Zhu JX, Chen TH. Montmorillonite-supported Magnetite nanoparticles for the removal of hexavalent chromium [Cr(VI)] from aqueous solutions. J. Hazard. Mater. 2009; 166(2–3):821–829. [PubMed: 19135796]
43. Leppert D. Heavy metal sorption with clinoptilolite zeolite: alternatives for treating contaminated soil and water. Min. Eng. 1990; 42(6):604–608.
44. Krishna BS, Murty DSR, Jai Prakash BS. Thermodynamics of Chromium(VI) Anionic Species Sorptiononto Surfactant-Modified Montmorillonite Clay. J, Colloid Interface Sci. 2000; 229:230–236. [PubMed: 10942564]
45. Smith E, Ghiassi K. Chromate removal by an iron sorbent: mechanism and modeling. Water Environ. Res. 2006; 78:84–93. [PubMed: 16553170]

Highlights

$MnFe_2O_4$ and Fe_3O4 were synthesized and investigated to remove chromium(III) and (VI) from solution.

The pH optimum binding for the chromium ions was determined to be at pH 3 and pH 5 for Cr(III) and Cr(VI).

The capacity of each material was determined under light and dark reaction conditions.

The thermodynamic parameters were determined for the sorption of Cr(III) and Cr(VI) to the two nanomaterials.

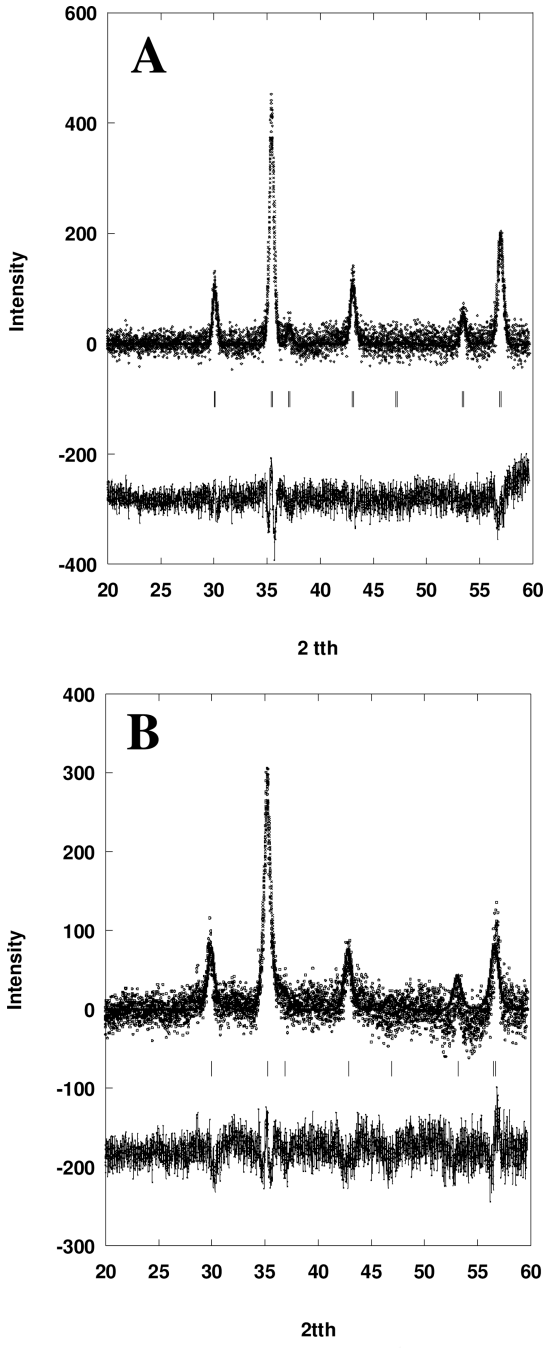

Figure 1.

A. XRD pattern and fitting for Fe_3O_4 nanomaterials as synthesized and the indexed diffraction peaks. **B.** XRD pattern and fitting for $MnFe_2O_3$ nanomaterials as synthesized and the indexed diffraction peaks.

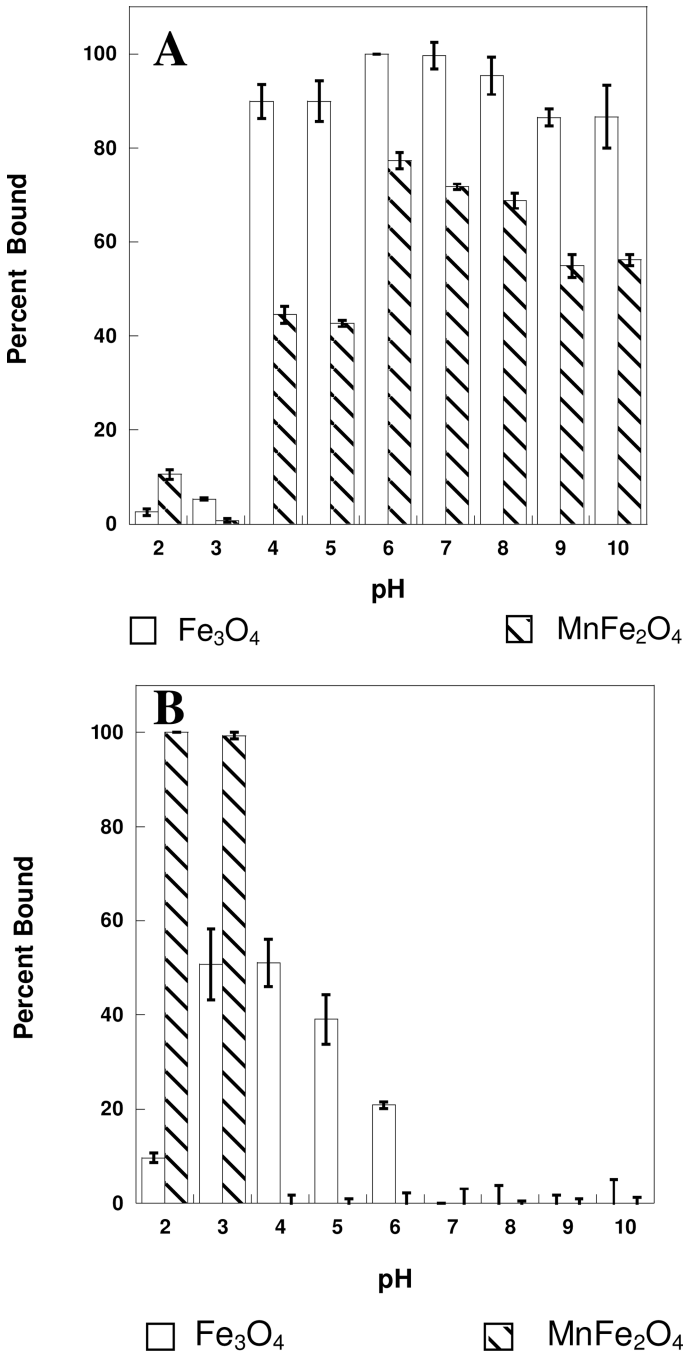

Figure 2.
pH profiles for the binding of chromium(III) to the Fe_2O_3 and $MnFe_2O_4$ nanomaterials (A) and chromium(VI) to the Fe_2O_3 and $MnFe_2O_4$ nanomaterial (B) from pH 2 through pH 10.

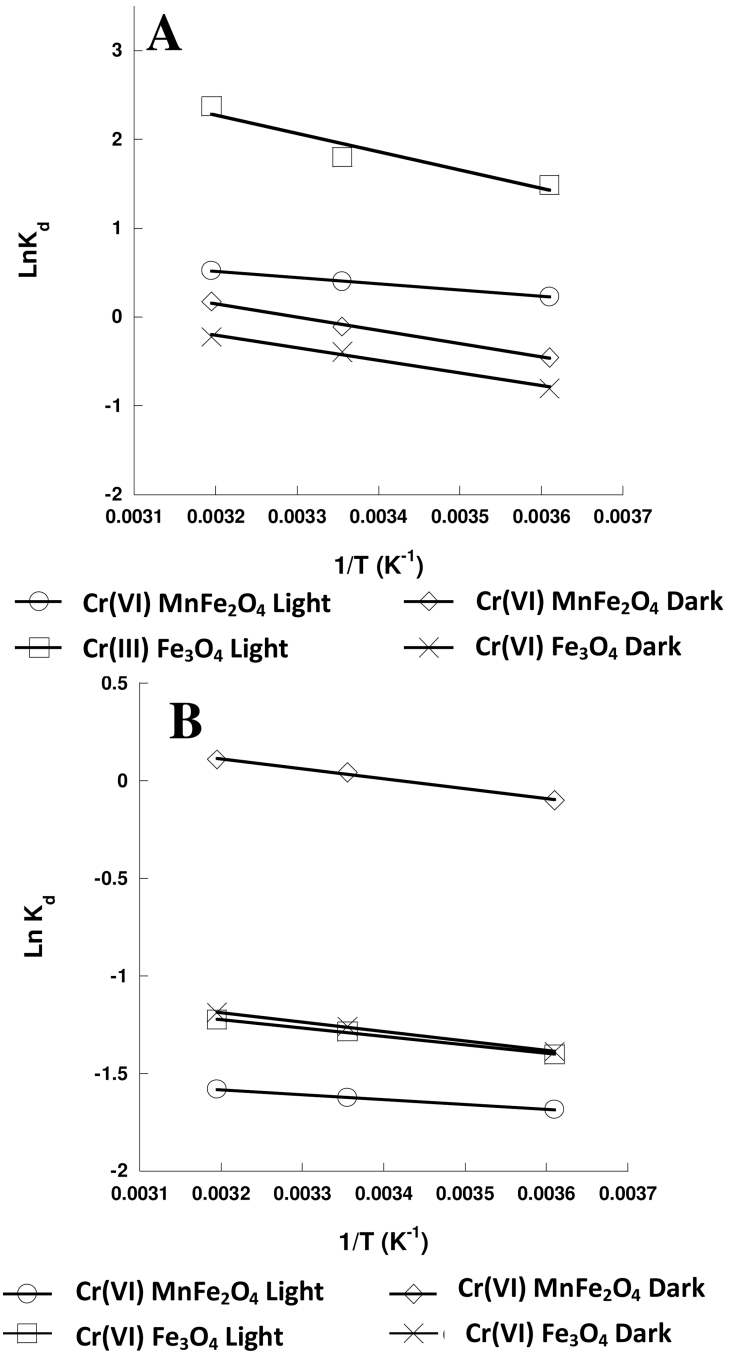

Figure 3.

A. Plot of Ln K_d versus T^{-1} for chromium(III) sorption to the $MnFe_2O_4$ and Fe_3O_4 nanomaterials under light and dark conditions. **B.** Plot of Ln K_d versus T^{-1} for chromium(VI) sorption to the $MnFe_2O_4$ and Fe_3O_4 nanomaterials under light and Dark conditions.

Table 1

ICP-OES Operational parameters used for the analysis of chromium concentrations in solution after reaction with the different nanoadsorbents.

Parameter	Setting
λ	267.716 nm
RF power	1500 W
Nebulizer	Minehard
Plasma Flow	15 L/min
Auxiliary Flow	0.2 L/min
Nebulizer Flow	0.55 L/min
Sample Flow	1.50 mL/min
Injector	2.0 mm Alumina
Spray Chamber	Cyclonic
Integration Time	10–20 seconds

Table 2

Capacities for Chromium(III) and Chromium(VI) binding to the studied nanomaterials under light conditions.

Material	Capacity (mg/g)	Error (± mg/g)
$MnFe_2O_4$ Chromium(III)	7.189	0.620
Fe_3O_4 Chromium(III)	10.638	1.303
$MnFe_2O_4$ Chromium(VI)	3.211	0.233
Fe_3O_4 Chromium(VI)	3.455	0.110

Table 3

Capacities for Chromium(III) and Chromium(VI) binding to the studied nanomaterials dark conditions.

Material	Capacity (mg/g)	Error (± mg/g)
$MnFe_2O_4$ Chromium(III)	5.736	0.413
Fe_3O_4 Chromium(III)	15.899	1.20
$MnFe_2O_4$ Chromium(VI)	3.868	0.032
Fe_3O_4 Chromium(VI)	8.547	0.054

Table 4

Calculated Gibbs free energy for the binding of chromium(VI) to the metal oxide nanomaterials under light(*) and dark (**) conditions.

Material (Temp K)	ΔG*(kJ/mol)	ΔG**(kJ/mol)
Fe_3O_4 (323)	−7.50	−7.60
Fe_3O_4 (298)	−7.33	−7.40
Fe_3O_4 (277)	−7.02	−7.06
$MnFe_2O_4$ (323)	−6.54	−11.07
$MnFe_2O_4$ (298)	−6.43	−10.90
$MnFe_2O_4$ (277)	−6.26	−10.52

Table 5

Calculated Gibbs free energy for the binding of chromium(III) to the metal oxide nanomaterials under light(*) and dark (**) conditions.

Material	ΔG* (kJ/mol)	ΔG**(kJ/mol)
Fe_3O_4 (323)	−17.16	−10.19
Fe_3O_4 (298)	−15.62	−9.72
Fe_3O_4 (277)	−14.79	−8.63
$MnFe_2O_4$ (323)	−12.18	−11.25
$MnFe_2O_4$ (298)	−11.86	−10.489
$MnFe_2O_4$ (277)	−11.40	−9.55

Table 6

Calculated apparent ΔH_{ads} for the binding of chromium(III) and chromium(VI) to different metal oxide nanomaterials under light(*) and dark(**) conditions.

Material	ΔH* (kJ/mol)	ΔH** (kJ/mol)
$MnFe_2O_4$ Chromium(III)	17.04	11.80
Fe_3O_4 Chromium(III)	5.84	12.55
$MnFe_2O_4$ Chromium(VI)	2.10	4.21
Fe_3O_4 Chromium(VI)	3.59	4.02

Table 7

Calculated apparent ΔS_{ads} for the binding of chromium(III) and chromium(VI) to different metal oxide nanomaterials under light(*) and dark(**) conditions.

Material	ΔS* (J/mol)	ΔS** (J/mol)
$MnFe_2O_4$ Chromium(III)	69.26	36.00
Fe_3O_4 Chromium(III)	22.95	41.40
$MnFe_2O_4$ Chromium(VI)	−1.31	2.99
Fe_3O_4 Chromium(VI)	−6.43	14.41